SAND--91-1474C

DE92 002360

SAND91/1474C

SHOCK-COMPRESSION PROPERTIES OF CERAMICS

D. Grady[a],
a. Sandia National Laboratories, Experimental Impact Physics Division 1543, Albuquerque, New Mexico, 87185-5800, U.S.A.

High-resolution, time-resolved shock compression measurements have been performed on high-strength monolithic ceramics to assess equation-of-state, phase transformation and flow properties. A substantial base of data has been obtained on a range of ceramics including aluminum nitride, aluminum oxide, boron carbide, silicon carbide, titanium diboride and zirconium dioxide. These data provide material response properties for nonlinear elastic compliance, pressure-induced phase transformation, shear strength and tensile fracture strength.

Keywords: Ceramic, Shock Wave, Phase Change, Elasticity.

INTRODUCTION

Certain of the intermetallic light weight compounds in polycrystalline ceramic form exhibit some of the highest strength properties measured on engineering materials. Limited plastic slip systems in these materials preclude lower stress plastic flow and dynamic strengths approach an appreciable fraction of their theoretical strengths [1].

Post-yield dynamic deformation of these ceramics under transient shock loading is complicated by the high-strength character of these materials. Although pervasive fine scale cataclastic fracture is generally preferred in material modelling [2], plastic flow through dislocation slip under the large confining pressures experienced in shock compression, either homogeneous or heterogeneous, cannot be ruled out.

Response to transient loads in these materials can be enriched by pressure induced phase transformation. Because of the high dynamic yield strengths, phase transformation and yield can intermix, further complicating transient equation-of-state response.

In the present investigation, dynamic material properties of high-strength ceramics have been studied using controlled impact methods. In the work reported, planar impact experiments, using high-resolution velocity interferometry diagnostics, have been performed on a selection of high-strength ceramics. The materials investigated include aluminum nitride, aluminum oxide, boron carbide, silicon carbide, titanium diboride and zirconium dioxide. Planar shock and release experiments have been performed to investigate Hugoniot properties, dynamic yield and post yield behavior, phase transformation, high pressure elasticity and tensile spall characteristics. Peak impact stresses range from below the Hugoniot elastic limit to approximately 60 GPa. Material deformation and equation-of-state properties are extracted from measured wave profile data through analytic and computational methods.

EXPERIMENTAL METHODS

In the present experimental study, gun impact methods and velocity interferometry (VISAR) diagnostics [3] are used to measure compression and release velocity profiles at an interface between the ceramic and a lithium fluoride window as indicated in Figure 1. The primary experimental results are the time-resolved interface velocity profiles. These profiles are used individually and collectively through both computational and analytic methods to extract desired dynamic material property data.

High-strength ceramics tested in the present program have been acquired from a number of sources. In several cases the same ceramic from several suppliers has been investigated allowing insightful comparisons of material

Figure 1. Experiment configuration for VISAR profile measurements.

properties variations due to differences in impurity content, microstructure and ceramic preparation.

HUGONIOT PROPERTIES

Principal Hugoniot data for the high strength ceramics determined from the VISAR data are shown in Figure 2. Small differences in Hugoniot behavior for the same ceramic from different suppliers are not indicated here. Softening of the Hugoniot response due to the onset of high-pressure phase transformation are indicated for aluminum nitride and zirconium dioxide. Similar softening in boron carbide is believed to be due to the loss of strength-supporting ability above the Hugoniot elastic limit of the material. The aluminum oxide tested in this study contained an initial porosity of about 10%.

The Hugoniot elastic limit (HEL) identifies the axial stress at which a solid, loaded in compression under constraint of uniaxial strain, can no longer support elastic distortion and begins to flow through plastic or cataclastic fracture processes. HEL data determined from the present wave profile experiments are summarized in Figure 3. For each material the reported HEL is based on an average of two or more experiments. The substantial difference in HEL values for the two boron carbides may reflect the substantially different grain sizes, (3 μm for the first material versus 10 μm for the second material). Higher impurity content in the latter material may also play a role. The HEL for silicon carbide is approximately twice the 8 GPa value reported by Gust et al [4]. It is

Figure 2. Hugoniot equation-of-state data for high-strength ceramics.

speculated that this is due to the substantially lower silica content of modern silicon carbides.

The modest HEL values for titanium diboride reported in Figure 2 belie the complex dynamic strength properties of this material as are discussed in the next section. The HEL of about 8 GPa for aluminum nitride is in good agreement with recent data of Rosenberg et al [5].

Figure 3. Hugoniot elastic limit properties for ceramics.

DYNAMIC STRENGTH

Dynamic yield strengths approaching an appreciable fraction of the theoretical strength are characteristic of the present ceramics. This is not necessarily a dynamic effect, however. Gilman [1] has noted that numerous compounds including many carbides, borides and oxides exhibit a marked resistance to plastic flow with energies near the bond strength required to move dislocations on glide planes.

Complexities in the dynamic yield and post-yield strength of ceramics is aptly illustrated in the behavior of the two carbides studied in the present work. Silicon carbide reveals an uncommonly high Hugoniot elastic limit (~15 GPa). Post-yield strength of silicon carbide, determined by comparison of Hugoniot uniaxial strain response and calculated hydrodynamic response, reveals neutral or increasing strength with subsequent deformation beyond the initial

dynamic yield. This is shown in Figure 4 where the dynamic shear strength at the Hugoniot state versus total shear strain is shown. Boron carbide, in contrast, exhibits the highest Hugoniot elastic limit measured in this work (~ 18 GPa). Subsequent deformation, however, shows a loss in strength supporting capability. Hugoniot and hydrodynamic response converge at stresses approaching about twice the Hugoniot elastic limit, indicating little or no strength at subsequent Hugoniot states (Figure 4). The contrast in dynamic strength characteristics of silicon carbide and boron carbide is further amplified in the release properties of these materials from the Hugoniot state. The release paths for silicon carbide indicate reverse yielding and the sustained strength characteristics of elastic-plastic material behavior. The unloading stress-volume paths for boron carbide closely parallel the calculated hydrodynamic behavior suggesting near fluid-like response with sustained strength loss.

Reasons for the differences in behavior between silicon carbide and boron carbide are uncertain. Motion fluctuations in observed wave profiles for boron carbide suggest that dynamic yield and flow in this material may be heterogeneous. Thus, the possibility exists for localized deformation under shock loading with accompanying softening due to thermal or structural mechanisms. In contrast, similar examination of wave profiles in silicon carbide indicate homogeneous flow on the microstructural scale. Loss of strength in boron carbide may also be related to the unusual boron carbide crystal structure and three-body covalent bonding in this material. The nature of this molecular structure is

Figure 4. Post-yield dynamic shear strength of silicon and boron carbide.

known to produce unusual behavior in other material properties of boron carbide [6].

The dynamic yield of titanium diboride also illustrates a complication in character not observed in other materials. Compressive wave profiles for titanium diboride reveal a softening of the axial modulus at two stress levels. The first softening (identified as the Hugoniot elastic limit in Figure 3) occurs at about 5 to 7 GPa; the second occurs at approximately 13 to 17 GPa. Although one or the other of these two yields has previously been tentatively interpreted as a stress-induced phase transformation [7], more recent static high-pressure studies have made this interpretation less likely. It is currently speculated that under shock-wave compression, titanium diboride undergoes a complex two-mechanism yield process. Examination of shock recovered specimens of titanium diboride by Vanderwalker and Croft [8] reveals dislocation basal and prismatic slip on crystal grains favorably oriented with respect to the shock wave. This suggests yield anisotropy in shock-loaded hexagonal titanium diboride. Lower yield at 5 to 7 GPa occurs only in preferred orientation grains and plastic strain saturation is quickly achieved. Lower yield is apparently insufficient to eliminate intrinsic ceramic porosity. Upper yield occurs at about 13 to 17 GPa. It is pervasive and is sufficient to collapse material porosity which occurs preferentially at grain triple points in the present materials. The occurrence of porosity collapse at upper yield is revealed in the present work through examination of shock data from two titanium diboride materials with differing initial densities.

HUGONIOT RELEASE PROPERTIES

Impact experiments are designed to provide for a controlled uniaxial strain unloading from the Hugoniot state. Because of the large amplitude of the elastic precursor wave reflected from the back of the impacting ceramic sample, an appreciable portion of initial unloading is from a centered simple release wave. The propagation of such waves can be investigated to determine the high-pressure compliance of the tested materials. When high-pressure equation-of-state and elasticity properties are sought the wave profile data must be critically examined. Because of the uniaxial nature of the shock load and release process, modulus data can be complicated by yield and deformation processes during release. Transit time through the ceramic specimen of the initial break of the release wave corresponds to the initial longitudinal modulus of the material at the Hugoniot state. The modulus is determined from the Lagrangian transit velocity C_l through,

$$K_l = \frac{\rho_o^2}{\rho} C_l^2. \tag{1}$$

Further, the initial slope of the release wave profile provides the longitudinal stress derivative of the modulus through,

$$K_l' = 2\frac{\rho_o}{\rho}\frac{dC_l}{du} - 1. \tag{2}$$

Data obtained from shock release wave profiles for silicon carbide are shown in Figure 5. The moduli data in Figure 5(a) determined from Equation (1) provide a stress derivative of $K_l' = 2.33$ and extrapolate reasonably well to the ultrasonic longitudinal modulus of silicon carbide. In Figure 5(b) the individual stress derivatives determined directly through Equation (2) are plotted and values are in good agreement with the slope of the data from Figure 5(a). A value of $K_l K_l'' = -24.9$ determined from Figure 5(b) is in reasonable agreement both in sign and magnitude with similar high pressure static data [9]. It is noted that the moduli and stress derivatives for high-pressure static and shock analysis are different.

Similar data for aluminum oxide and zirconium dioxide are shown in Figure 6 and Figure 7. Values of K_l' determined from the slope of the moduli data are 2.46 and 1.85, respectively. Data for aluminum oxide extrapolate well to the ultrasonic value while that for zirconium dioxide does not. In contrast to silicon carbide, data for K_l' determined from Equation (2) are large (~ 7 to 15) and the trend with Hugoniot stress is different.

Figure 5. Hugoniot release moduli and derivatives for silicon carbide.

Figure 6. Hugoniot release moduli and derivatives for aluminum oxide.

Data for silicon carbide for both K_l and K_l' determined from the arrival and structure of the release wave (Equation 1 and 2) appear to reflect elasticity properties of the material at pressure. Similarly, data for K_l for both aluminum oxide and zirconium dioxide probably provide useful stress-dependent elastic modulus data. Aluminum oxide and zirconium dioxide data for K_l' in Figures 6 and 7, however, are more likely reflecting complex structural yield and flow properties of the material. The present release data are preliminary. More work is needed to assess usefulness of the Hugoniot release data and sort out the relative effects of elasticity and strength in evaluation of the release wave structure.

Figure 7. Hugoniot release moduli and derivatives for zirconium dioxide.

PHASE TRANSFORMATION

In shock-wave studies it has become common to associate first convexity in the compressive wave profile with onset of shear yielding through dislocation or fracture mechanisms and subsequent convexities with polymorphic phase transformations. In the present high-strength ceramics with large barriers to dislocation activation and slip it is not clear that onset of shear deformation need necessarily precede pressure-induced lattice instability. Further, complexities in the shear deformation process such as the upper and lower yields identified in titanium diboride contribute additional complications in identification of pressure-induced phase transformation in shock-wave studies.

In certain materials, evidence never-the-less supports shock-induced phase transformation. This is the case for several of the ceramics investigated in the present study. In aluminum nitride VISAR particle velocity profiles reveal clear evidence for two anomalies in the shock compressibility of this material. The first occurs at approximately 8 GPa with a following wave velocity close to the bulk velocity of the material suggesting initial shear yielding at this level with subsequent normal elastic-plastic characteristics. The second occurs at approximately 20 GPa compressive stress. The following shock wave is slow (~4 km/s). The stress-volume Hugoniot inferred from the wave-profile data indicate a transformation volume strain of about 20%. Shock transformation of aluminum nitride at this stress level has previously been reported by Kondo et al [10]. The results are in accord with recent static studies of Vollstadt et al [11]. Transformation to cubic structure is observed in that work at about 16 GPa static pressure with a volume change comparable to that observed in shock-wave experiments.

Transformation under shock-wave compression is also indicated in zirconium dioxide [12]. Anomalies in the compressive wave profile are observed at about 15 to 18 GPa and again at about 30 to 32 GPa. Whether onset of deformation plasticity is responsible for the lower yield in tetragonal zirconia is difficult to establish. Shock velocity of the second wave is somewhat faster than expected for ideal plasticity, although this conclusion is dependent on the compression nonlinearity assumed for the material. Also, the lower yield occurs suspiciously close to the 14 to 16 GPa transition from tetragonal to orthorhombic structure observed in static experiments by Ohtaka and Kume [13]. Phase transition at 30 to 32 GPa under shock compression appears reasonable. Densification onset at this second yield is more pronounced.

Phase transformation may also be indicated under shock compression below the 15 to 18 GPa first compressive yield. No signature of a transformation is indicated in the compressive waves in experiments performed to Hugoniot stresses of 11 to 13 GPa. This Hugoniot stress level is below the Hugoniot elastic limit reported for zirconium dioxide in Figure 3. Release wave modulus

Figure 8. Release wave structure in zirconium dioxide.

data, however, do not extrapolate to the low pressure longitudinal modulus (Figure 7). Release profiles in this range shown in Figure 8 suggest possible formation of a rarefaction shock wave. Further, the high values for the finite amplitude Hugoniot elastic wave velocity relative to the ultrasonic longitudinal velocity [14] also attest to a possible phase change in tetragonal zirconia below the 15 to16 GPa first compressive yield.

REFERENCES

1. J. J. Gilman, J. Appl. Phys. **41** (1970) 1664
2. F. L. Addessio and J. N. Johnson, J. Appl. Phys. **67** (1990) 3275
3. L. M. Barker and R. E. Hollanbach, J. Appl. Phys. **43** (1972) 4669
4. W. H. Gust, A. C. Holt and E. B. Royce, J. Appl. Phys. **44** (1973) 550
5. Z. Rosenberg, N. S. Brar and S.J. Bless, J. Appl. Phys. **70** (1991) 167
6. D. Emin, Phys. Today **1** (1987) 1
7. D. E. Grady, in Shock Waves in Condensed Matter - 1991, eds. S. C. Schmidt et al. (to be published)
8. D. M. Vanderwalker and W. J. Croft, J. Mater. Res. **3** (1988) 761
9. L. C. Chhabildas and A. L. Ruoff, J. Appl. Phys. **47** (1976) 4182
10. K. Kondo, A. Sawaoka, K. Sato and M. Ando, in Shock Waves in Condensed Matter - 1981, eds. W. Nellis et al. (Amer. Inst. Phys., 1982) p.325
11. H. Vollstadt, E. Ito, M. Akaishi, S. Akimoto and O. Fukunaga, Proc. Japan Acad. **66** (1990) 7
12. D. Grady and T. Mashimo, J. Appl. Phys. (to be published)
13. O. Ohtaka and S. Kume, J. Am. Ceram. Soc. **71** (1988) C-448
14. T. Mashimo, J. Appl. Phys. **63** (1988) 4747

PLANAR IMPACT EXPERIMENT

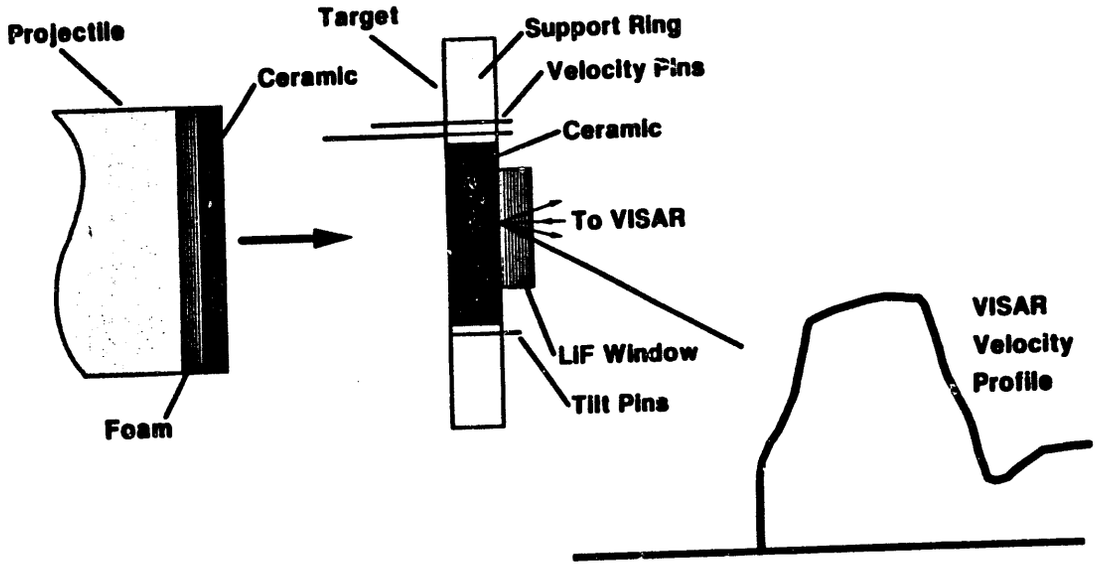

90H1000.18

64% reduction of original

FIGURE # 1

U4:[DEGRADY.VISARDATA.CERAMIC]HUGPV.CMD

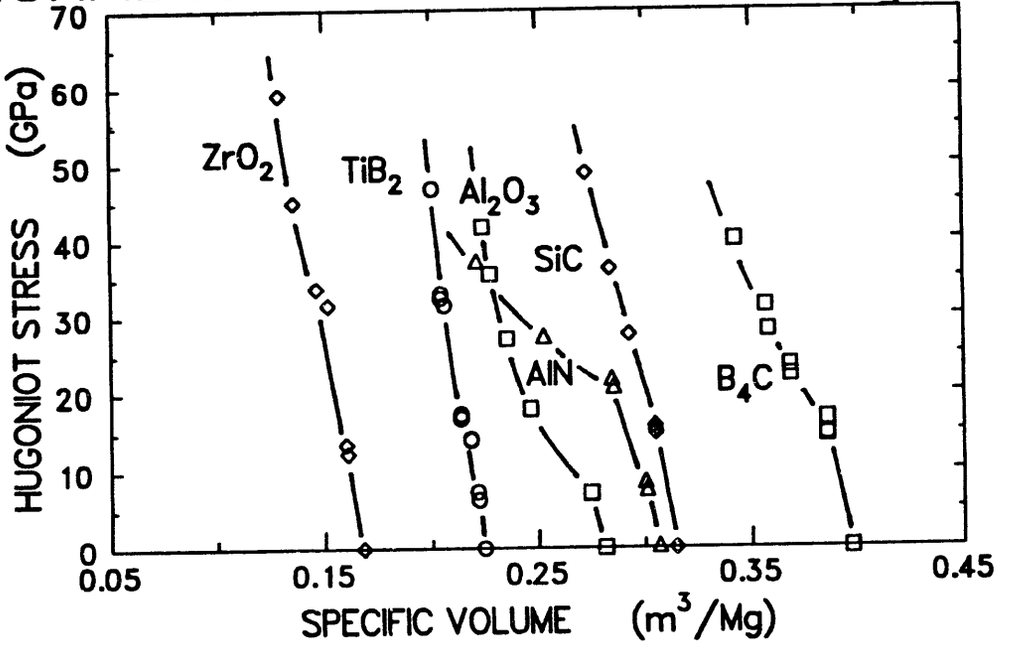

FIGURE 2

u4/degrady/visardata/ceramic/helfig.cmd

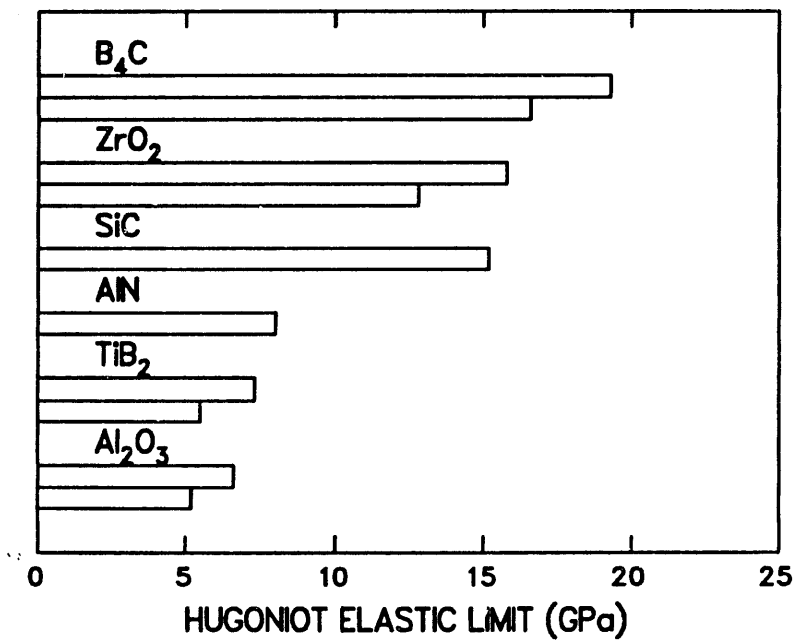

FIGURE 3

u4/degrady/visardata/ceramic/shearsb.cmd

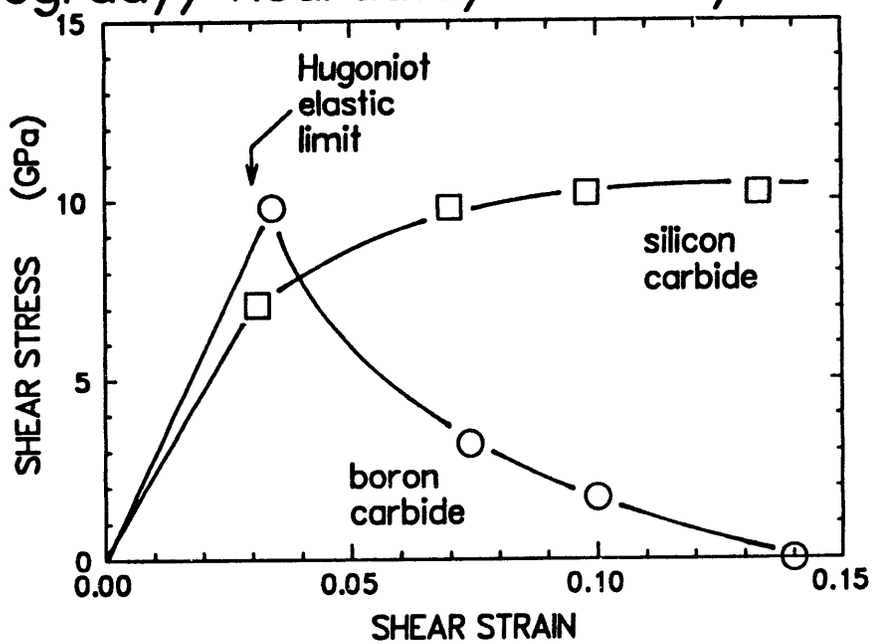

FIGURE 4

u4/degrady/visardata/ceramic/sic/kfig.cmd

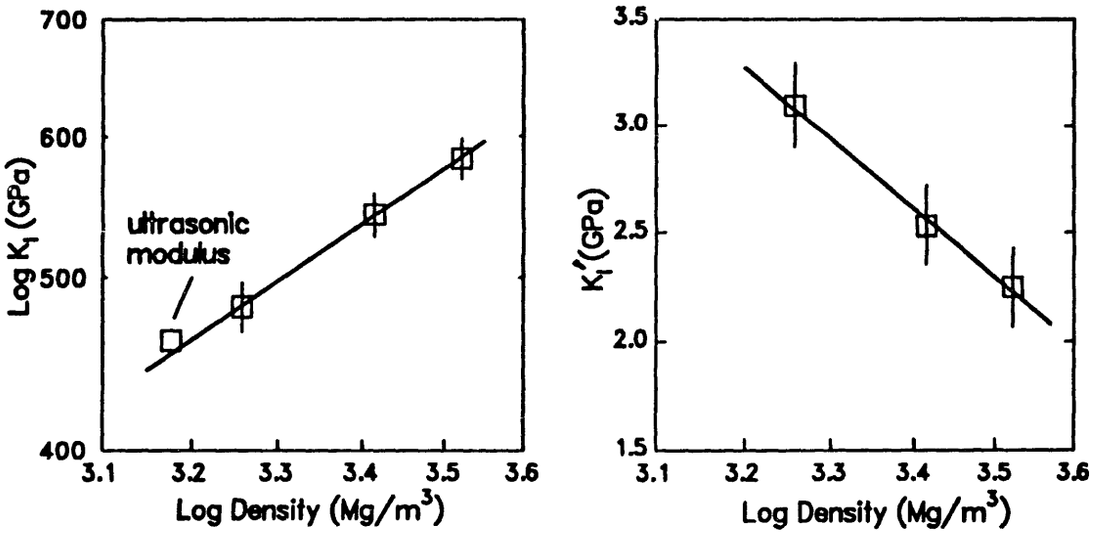

Figure 5

u4/degrady/visardata/ceramic/al2o3/kfig.cmd

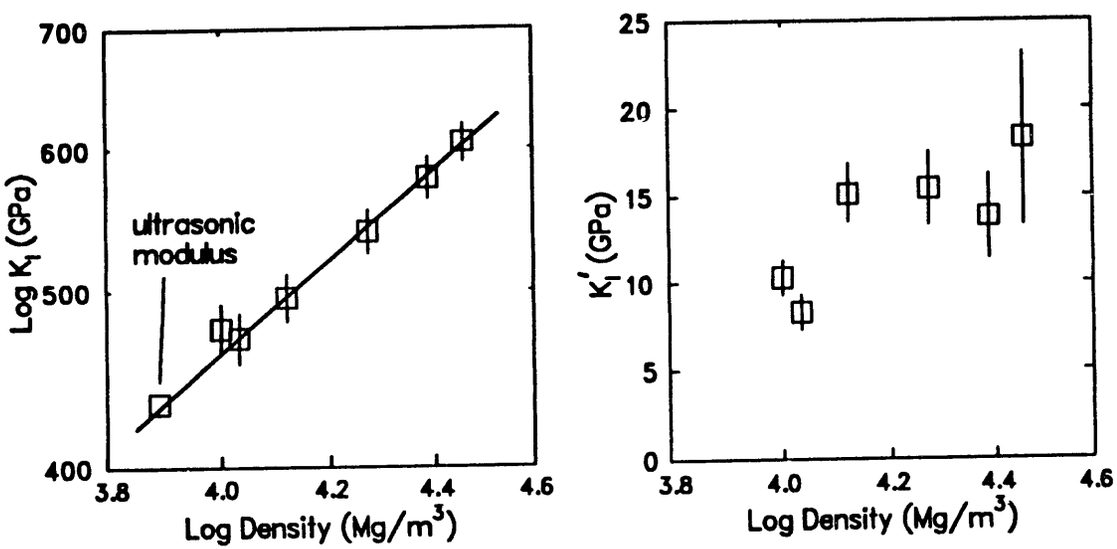

Figure 6

u4/degrady/visardata/ceramic/zro2/kfig.cmd

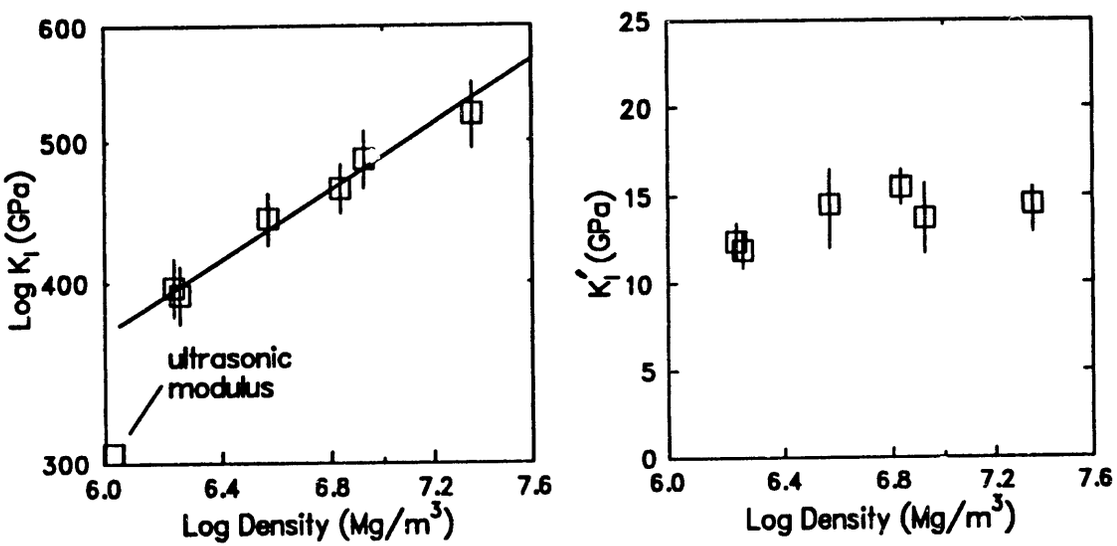

Figure 7

u4/degrady/visardata/ceramic/ce39fig.cmd

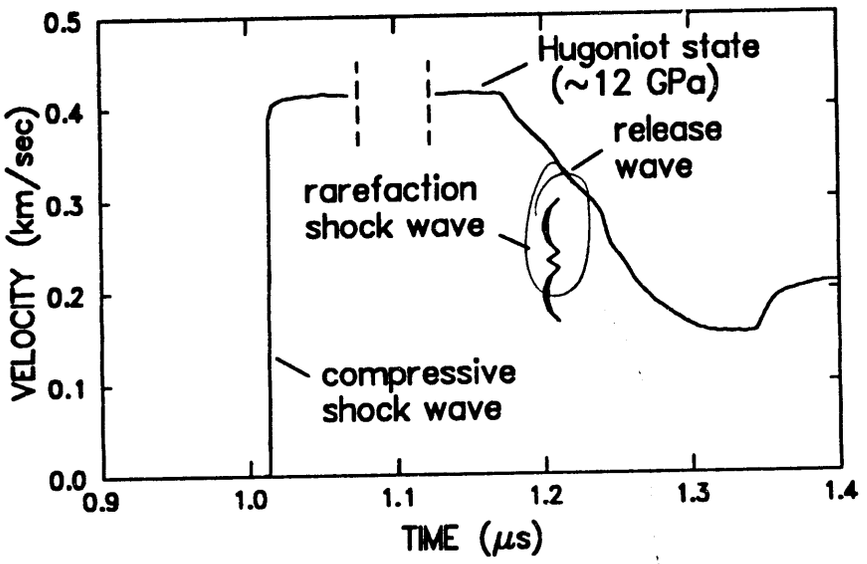

Is this right?

Figure 8

END

DATE FILMED

12/16/91